DLW-CI: A Dynamic Likelihood-Weighted Cooperative Infotaxis Approach for Multi-Source Search in Urban Environments Using Consumer Drone Networks

Xiaoran Zhang†, Yatai Ji†, Yong Zhao, Chuan Ai, Bin Chen*, and Zhengqiu Zhu*

***Abstract*—Consumer-grade drones equipped with low-cost sensors have emerged as a cornerstone of Autonomous Intelligent Systems (AISs) for environmental monitoring and hazardous substance detection in urban environments. However, existing research primarily addresses single-source search problems, overlooking the complexities of real-world urban scenarios where both the location and quantity of hazardous sources remain unknown. To address this issue, we propose the Dynamic Likelihood-Weighted Cooperative Infotaxis (DLW-CI) approach for consumer drone networks. Our approach enhances multi-drone collaboration in AISs by combining infotaxis (a cognitive search strategy) with optimized source term estimation and an innovative cooperative mechanism. Specifically, we introduce a novel source term estimation method that utilizes multiple parallel particle filters, with each filter dedicated to estimating the parameters of a potentially unknown source within the search scene. Furthermore, we develop a cooperative mechanism based on dynamic likelihood weights to prevent multiple drones from simultaneously estimating and searching for the same source, thus optimizing the energy efficiency and search coverage of the consumer AIS. Experimental results demonstrate that the DLW-CI approach significantly outperforms baseline methods regarding success rate, accuracy, and root mean square error, particularly in scenarios with relatively few sources, regardless of the presence of obstacles. Also, the effectiveness of the proposed approach is verified in a diffusion scenario generated by the computational fluid dynamics (CFD) model. Research findings indicate that our approach could improve source estimation accuracy and search efficiency by consumer drone-based AISs, making a valuable contribution to environmental safety monitoring applications within smart city infrastructure.**

***Index Terms*—Consumer-grade drones, multi-drone collaboration, multi-source search, dynamic likelihood weight, parallel particle filters, smart city.**

I. Introduction

DRIVEN by advancements in consumer electronics, Autonomous Intelligent Systems (AISs) have transformed environmental monitoring and safety applications within smart cities [1]. The serious threats posed by hazardous substance leaks in urban environments highlight the critical need for rapid and accurate source localization systems that can be deployed at scale using accessible consumer technology. To effectively mitigate such threats, consumer-grade drones [2] equipped with gas sensors, cameras, and communication modules have emerged as ideal platforms for autonomous source search and localization tasks [3], as illustrated in Fig. 1.

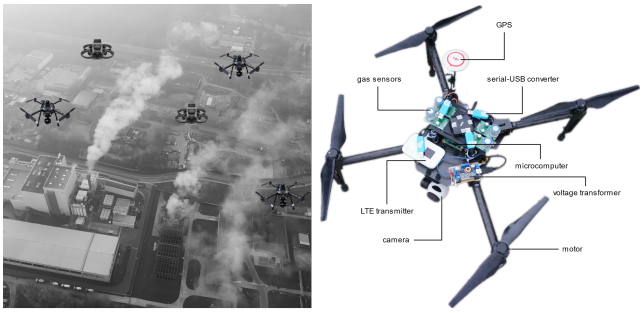

Fig. 1. An illustrative source search scenario supported by comsumer-grade drones in real-world.

The deployment of multiple mobile sensor-based platforms for autonomous source localization has emerged as a key research focus in the field. It refers to multiple mobile devices (such as consumer drones equipped with multiple sensors) moving autonomously toward the source of a leak based on environmental data collected by the sensors and ultimately declaring the location of the source in a collaborative manner [4]. In recent years, consumer drones have been widely adopted in source search tasks [5] due to their advantages in rapid deployment, coverage capacity, and relatively low cost, making them accessible components for civilian AISs in smart city applications [6], [7].

A. Autonomous Search Strategies

Autonomous search strategies can be broadly classified into two categories: bio-inspired strategies and cognitive strategies [8], [9], [10], [11]. (1) Bio-inspired strategies replicate animal search behaviors, such as lobsters using their antennae for foraging [12], silkworms tracking pheromone clouds to locate mates [13], and dung beetles employing zigzag movements within odor clouds [14]. These bioinspired methods are computationally efficient due to their theoretical simplicity. However, their performance is inherently limited by turbulence [10], [15], as these methods do not fully utilize the available

This study is supported by Youth Independent Innovation Foundation of NUDT (ZK-2023-21) and National Natural Science Foundation of China 62173337. (*Xiaoran Zhang and Yatai Ji contributed equally to this work.*) (*Corresponding author: Bin Chen and Zhengqiu Zhu*).

Xiaoran Zhang, Yatai Ji, Yong Zhao, Chuan Ai and Zhengqiu Zhu are with the College of Systems Engineering, National University of Defense Technology, Changsha 410073, Hunan Province, China. (email: zhangxiaoran@nudt.edu.cn; jiyatai_1209@nudt.edu.cn; zhaoyong15@nudt.edu.cn; aichuan@nudt.edu.cn; zhuzhengqiu12@nudt.edu.cn).

Bin Chen is with the Institute of Intelligent Computing, University of Electronic Science and Technology of China (UESTC), Chengdu 611731, Sichuan Province, China. (email: nudtcb9372@gmail.com).

information when determining subsequent movements. (2) Another category of autonomous search strategies, referred to as cognitive strategies, is information-driven [15] and has proven effective for performing source search tasks in turbulent environments [16], [17], [18], [19], [20], [21]. Cognitive strategies involve the searcher continuously collecting information during the search process to improve the estimation of the source term (e.g. source location, release strength, etc.). This refined estimation then guides the searcher's subsequent actions until the source is successfully identified. While these approaches are computationally more demanding, they can be optimized for consumer-grade hardware through lightweight implementations and distributed processing techniques [22].

B. Multi-source Search Approaches

However, the aforementioned search strategies are not directly applicable to multi-source scenarios. When guided by these strategies, the search often identifies a local optimum corresponding to one source, limiting the ability to continue searching for other potential sources. This limitation is particularly problematic in smart city applications where multiple pollution sources, gas leaks, or other environmental hazards may simultaneously exist and affect residents. To achieve more accurate multi-source localization using consumer AISs, existing research has primarily focused on two aspects: multi-drone search for source locations [23], [24], [25], [26], [27], and multi-drone estimation of the source distribution field [28], [29]. The former involves multi-source search by drone collaboration to declare the source locations, while the latter estimates the multi-source term and ultimately generates a concentration distribution map. Both approaches possess distinct advantages for consumer applications, particularly when accounting for the energy efficiency and communication constraints inherent to affordable sensing platforms.

In research on multi-drone search for source locations, Cabrita et al. [23] proposed treating declared sources as invisible, allowing drones to continue searching for additional sources without getting stuck in local optima. Ji et al. [27] proposed a role-based framework assigning distinct roles to ground robots and consumer drones: 'collectors' map the concentration distribution, while 'identifiers' use this map to navigate towards the source. Swarm intelligence approaches, on the other hand, are well-suited for multi-source scenarios. Zou et al. [25] introduced a multi-source search method inspired by ant colony optimization, mimicking the foraging behaviors of ants. Similarly, Zhang et al. [24] proposed a niching particle swarm optimization (niching PSO) algorithm that dynamically forms and disperses subgroups to locate multiple sources. In contrast, research on multi-drone estimation of source distribution fields focuses on the designs of drones' perception, control, and estimation mechanisms. Leong et al. [28] developed a concentration field estimation method using binary sensors with an active sensing mechanism to adaptively select measurements. While Tran et al. [29] proposed a multi-drone mobility strategy integrating active perception and sequential Monte Carlo fusion to localize and map multiple sources in leakage scenarios.

C. Challenges

A review of multi-source localization reveals critical gaps: existing source search methods lack source term estimation in multi-source scenarios, causing consumer drones to underutilize concentration data, leading to suboptimal movement and wasted energy. Conversely, concentration field fitting methods, while leveraging source term estimation, often struggle to accurately map concentration distributions when multiple sources are present. To achieve efficient and accurate multi-source localization with consumer-grade drones, it is essential to explore the effective integration of source search and source term estimation in multi-source scenarios. In this regard, we face the following challenges:

- In multi-source scenarios, observations collected by consumer drones represent the cumulative results of all sources, making it difficult to isolate the contribution of any single one. Consequently, directly applying the Poisson observation model to update particle weights becomes ineffective, hindering accurate localization of the unknown sources.
- In multi-source scenarios, when multiple consumer drones search for unknown sources, they tend to cluster around a single source due to limited communication and coordination capabilities, failing to effectively search for other unknown sources and wasting precious battery life.

D. Contributions

To address these challenges, we propose the Dynamic Likelihood-Weighted Cooperative Infotaxis (DLW-CI) approach for consumer drone networks. In this approach, we design a multi-drone collaborative source estimation method and integrate it with the Infotaxis strategy [18], enabling coordinated estimation and search by effectively pairing consumer drones with potential sources. Extensive experiments—including Monte Carlo studies in both obstacle-free and obstructed environments, as well as a case study—demonstrate the superiority of the proposed method over baseline models. The main contributions of this work are summarized as follows:

- This paper introduces DLW-CI, an information-driven approach for solving the multi-source search problem with consumer drone networks. By redesigning the source estimation process and improving drone cooperation, our method increases the efficiency and success rate of multi-source search. Research findings show that DLW-CI offers valuable benefits for environmental safety monitoring applications in smart cities.
- To address the first challenge, this paper introduces a source term estimation method that employs multiple parallel particle filters to identify potential unknown sources within a search scene. By aggregating the outputs of individual filters, the source term estimation is iteratively refined and updated, substantially improving estimation accuracy in multi-source scenarios.
- To address the second challenge, this paper introduces a cooperative mechanism based on dynamic likelihood weighting. By incorporating this weight into source term

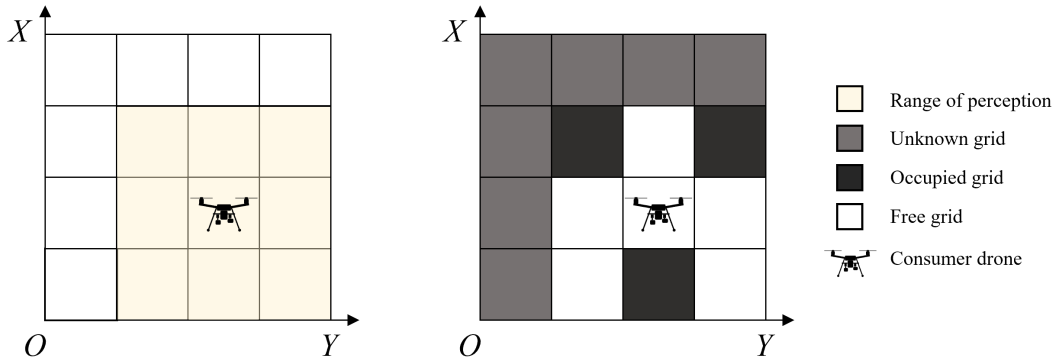

(a) Obstacle-free environment (b) Obstacle environment

Fig. 2. Environment representation. (**a**) Source search in the obstacle-free environment. The pale yellow grid indicates the range of the consumer drone's perception of the surrounding area; (**b**) Source search in the obstacle-present environment. Gray, black, and white grids represent unknown, occupied, and free grids, respectively. Free grids represent the area where the consumer drone can navigate. Occupied grids denote the area where obstacles exist. Unknown grids signify areas that remain undetected by the consumer drones.

estimation process, consumer drones can pair more effectively with unknown sources, improving coverage in multi-source scenarios while optimizing energy usage and communication overhead.

- Extensive experiments across obstacle-free, obstacle-present, and obstacle-influenced diffusion scenarios demonstrate the method's performance and robustness in typical urban environments. Results show that the DLW-CI approach increases the success rate by an average of 37% over the state-of-the-art niching PSO baseline when locating 2, 3, and 4 diffusion sources in obstacle-free scenarios. Notably, DLW-CI can successfully perform multi-source search with considerable performance in environments containing obstacles, whereas baseline methods are unable to achieve this.

The remainder of this paper is organized as follows: Section II describes the multi-source search problem and introduces the environment and sensor models. Section III presents the proposed DLW-CI approach, detailing the redesigned source term estimation method and a cooperative mechanism. Section IV provides two illustrative runs and reports extensive experiments to explore DLW-CI's performance, along with a case study in a realistic diffusion scenario. Finally, Section V summarizes the conclusions.

II. Problem Formulation

A. Multi-source search problem

The source search problem addressed in this paper involves guiding the consumer drones to localize multiple sources in both obstacle-free environments and obstructed environments, as shown in Fig. 2. Multiple sources, denoted as $S = \{s_1, s_2, \cdots, s_{N_s}\}$, continuously emit gas molecules with a finite lifetime τ, where N_s represents the number of sources. We use $s_i^{pos} = \{s_i^x, s_i^y\}$ to denote the location of each source and s_i^{str} as its release strength, where $i \in [1, N_s]$. During the source search process, the consumer drone networks collect measurements to estimate the source term parameter $\theta_s = \{(s_i^{pos}, s_i^{str})\}_{i=1}^{N_s}$. Considering that the gas molecule is advected by a mean wind with speed v and direction ϕ_v, the gas concentration released by the source s_i at position $d = \{x, y\}$ is formulated according to the steady-state convective diffusion equation [30]:

$$c_i(d|\theta_s^i) = \frac{s_i^{str}}{4\pi\sigma||d - s_i^{pos}||} \times exp^{\frac{-(x-s_i^x)v\sin\phi_v}{2\sigma}} exp^{\frac{-(y-s_i^y)v\cos\phi_v}{2\sigma}} exp^{\frac{-||d-s_i^{pos}||}{\lambda}}, \tag{1}$$

where $\lambda = \sqrt{\frac{\sigma\tau}{1+v^2\tau/4\sigma}}$, σ is the effective diffusion coefficient and τ is the gas molecule lifetime. The gas concentration in the multi-source scenario is then given by:

$$c(d|\theta_s) = \sum_{i=1}^{N_s} c_i(d|\theta_s^i). \tag{2}$$

Assuming that the gas effective diffusion coefficient σ, gas molecule lifetime τ, wind speed v, and wind direction ϕ_v are known, the number of sources N_s remains unknown. The parameter to be estimated during the gas source search process is the source term parameter $\theta_s = \{(s_i^{pos}, s_i^{str})\}_{i=1}^{N_s}$.

The goal of the multi-source search task is to guide the drones to traverse the environment while continuously collecting gas concentration measurements along its path to achieve an accurate estimation of the source parameters θ_s. In the following, we will provide a detailed overview of the environmental model and the drone's gas sensor model.

B. Environment and sensor models

1) Environment representation: As illustrated in Fig. 2, the two-dimensional source search environments consist of obstacle-free and obstructed scenarios. In an obstacle-free environment, the consumer drone does not need to consider obstacle avoidance. In contrast, for obstacle-present environments, we use an occupancy grid map to represent the environment, without accounting for the specific shapes of the obstacles.

The occupancy grid map is initially unknown to the consumer drone. As the drone navigates the environment, it senses the surrounding areas and progressively explores the map. Consequently, the map can be divided into two regions: known (explored) and unknown (unexplored). For the sake of simplification, we assume that the consumer drone can only move between two connected free grids and has a limited sensing range, which is eight pale yellow grids, as shown in Fig. 2(a). The states (free or occupied) of the grids within the perception range are known to the drone. This can be obtained through onboard sensors such as depth cameras or 2D rangefinders [31], [32].

2) Gas sensor model: As the drone moves along a path, its onboard gas sensor measures the gas concentration at each location. During the source search, the sensor needs to detect the signal within a limited time [18]. Berg et al.[33] studied the chemoreception process of using a spherical sensor with a radius a under limited measurement time and concentration conditions. Similar to this process, we utilize the Smoluchowski equation [34] to convert the gas concentration $c(d|\theta_s)$ at position d into the average number of contacts between the sensor and gas molecules per unit time:

$$N_s(d|\theta_s) = 4\pi\sigma \cdot a \cdot c(d|\theta_s). \tag{3}$$

In real environments, turbulence influences the gas diffusion, leading to a disturbance in the concentration field [16]. To account for this significant factor, we introduce a Poisson observation model to simulate the drone's perception of the diffusion environment under turbulent effects [19], with $N_s(d|\theta_s)$ serving as the intensity of the Poisson process. Then, the probability of the drone contacting the gas molecules r_{obs} times per unit time at position d is given by:

$$P(r_{obs}|\theta_s) = \frac{N_s(d|\theta_s)^{r_{obs}}}{r_{obs}!} e^{-N_s(d|\theta_s)}. \tag{4}$$

By generating random numbers following a Poisson distribution [18], the potential gas contacts at any position of the scenario can be generated as shown in Fig. 3(b). The turbulent effects evidently result in a more diversified distribution of the drone's observation values.

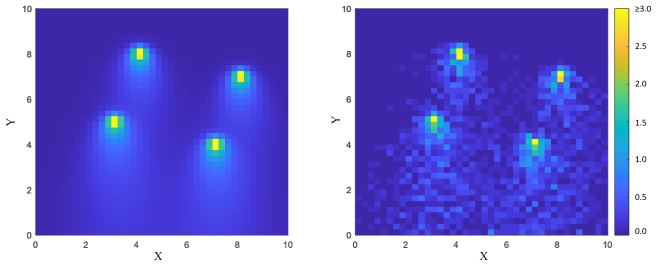

(a) Multi-source diffusion scenario (b) Multi-source perception scenario

Fig. 3. A multi-source diffusion scenario. (**a**) Example of a scenario with four diffusion sources; (**b**) Example of a diffusion scenario considering the effects of turbulence.

III. The DLW-CI approach

The proposed Dynamic Likelihood-Weighted Cooperative Infotaxis approach, illustrated in Fig. 4, integrates source term estimations with a cooperative mechanism for multi-source localization. First, parallel particle filters approximate source term estimations via Gaussian fitting, while acceptance degree (i.e. dynamic likelihood weight) is calculated through inter-drone parameter sharing. Collaborative drones then combine real-time observations with historical predictions, enabling Bayesian inference to update source term estimates from prior to posterior distributions. The updated estimates guide drone navigation using an Infotaxis reward function. This process repeats until the termination criteria are met.

A. Source term estimation based on parameter aggregation

In the cognitive strategy, the source search process is modeled as a Partially Observable Markov Decision Process (POMDP) [35]. The process consists of three core elements: information state, set of available actions, and reward function. At each step, the information state is updated based on the sensor data, driving the drones to choose the most suitable action from a set of available options. After obtaining new sensing information, the drone repeats this decision-making process until the source is accurately declared.

In this section, we define the information state of the POMDP as the posterior probability density function of the source term parameters, which is updated using the Bayesian method [36]. For the purpose of multi-source search, we assume that each drone has a pairwise estimated correspondence with an unknown source, and the number of drones is no less than the number of unknown sources, i.e, $N_r \geq N_s$. Therefore, the source term parameter θ_k^i estimated by the drone i at step k can be represented by the probability density function $P(\theta_k^i|I_k^i)$, where $I_k^i = \{r_{i,1}^{obs}, r_{i,2}^{obs}, \ldots, r_{i,k}^{obs}\}$ denotes all the observations up to step k. When the drone collects new information, the probability distribution of the source term parameter is updated using the Bayesian formula:

$$P\left(\theta_k^i|I_k^i\right) = \frac{P\left(\theta_{k-1}^i|I_{k-1}^i\right) P\left(r_{i,k}^{obs}|\theta_k^i\right)}{P\left(r_{i,k}^{obs}|I_{k-1}^i\right)}, \tag{5}$$

where $P\left(r_{i,k}^{obs}|I_{k-1}^i\right)$ is a normalization factor, formulated as:

$$P\left(r_{i,k}^{obs}|I_{k-1}^i\right) = \int P\left(\theta_{k-1}^i|I_{k-1}^i\right) P\left(r_{i,k}^{obs}|\theta_k^i\right) d\theta_k^i. \tag{6}$$

The prior probability distribution $P(\theta_{k-1}^i|I_{k-1}^i)$ is generated based on prior information. If no prior information is available, a uniform distribution is often selected. In the subsequent iterations, the prior probability distribution is replaced by the posterior probability distribution obtained from the previous step. The probability $P\left(r_{i,k}^{obs}|\theta_k^i\right)$ of the observation $r_{i,k}^{obs}$ is jointly determined by the convection-diffusion model and the Poisson observation model, which can be computed using Formula (4).

Since Formula (5) is nonlinear and challenging to solve using functional expressions, the sequential Monte Carlo

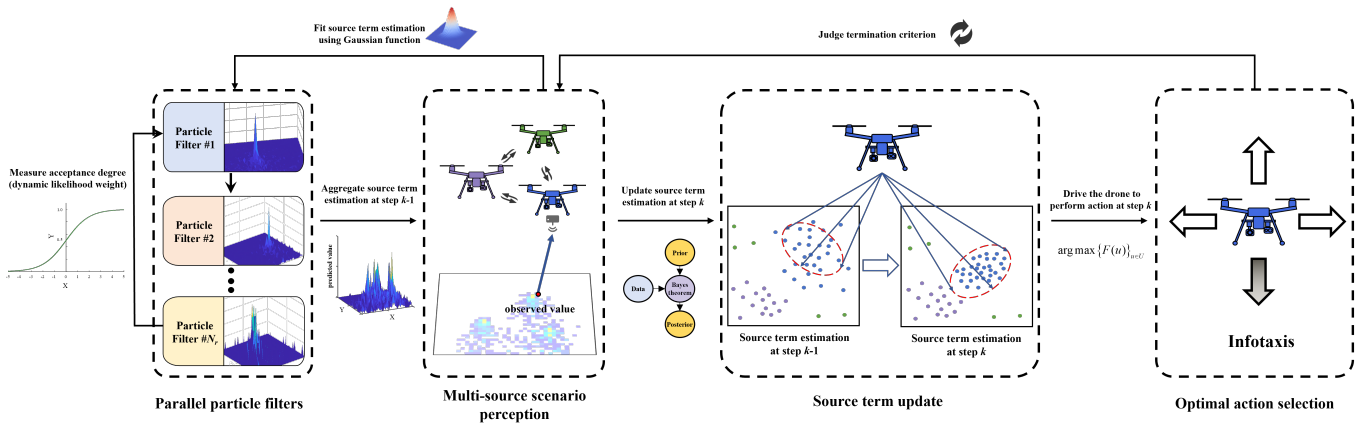

Fig. 4. The workflow of the DLW-CI approach integrates four sequential modules: **(1) Parallel particle filters:** the dynamic likelihood weight is computed through inter-drone parameter sharing. By aggregating the outputs of multiple particle filters, the predicted value is calculated. **(2) Multi-source scenario perception:** the drone obtains the observed value by perceiving in the multi-source scenario while utilizes the Gaussian function to fit the source term estimation of the previous step for parameter aggregation; **(3) Source term update:** the predicted and observed value are used to refine the source term estimation from prior to posterior based on the Bayes theorem; **(4) Optimal action selection:** the drone's next action is selected to maximize the reward function of Infotaxis. The cyclic process iterates until the termination criteria are met.

framework based on the particle filter is employed to approximate the estimation of source terms [19]. Specifically, the probability density function $P(\theta_k^i|I_k^i)$ is approximated by a set of N_p weighted samples (particles) $\{(\theta_k^{i,n}, w_k^{i,n})\}_{1\le n\le N_p}$ as:

$$P(\theta_k^i|I_k^i) \approx \sum_{n=1}^{N_p} w_k^{i,n}\delta(\theta - \theta_k^{i,n}), \tag{7}$$

where $\theta_k^{i,n}$ represents a point estimation of the source term parameter for the n_{th} particle of the drone i at step k, $w_k^{i,n}$ denotes the corresponding weight, which is normalized ($\sum_{n=1}^{N_p} w_k^{i,n} = 1$), and $\delta(\cdot)$ is the Dirac delta function.

To enable effective pairing between drones and sources in multi-source scenarios, we use multiple parallel particle filters to estimate the potential unknown sources. The particle filters are updated by aggregating the shared source terms, enabling each drone to conduct a targeted search for an individual unknown source.

To update the particle weights representing the estimation of the single-source term, the predicted value $[r_{i,k}^{obs}]_{pred}$ at the sampling position $r_{i,k}^{pos}$ is presented as:

$$[r_{i,k}^{obs}]_{pred} = 4\pi\sigma\cdot a\left\{c_i(r_{i,k}^{pos}|\theta_{k-1}^{i,n}) + \sum_{j=1,j\neq i}^{N_r} c_j(r_{i,k}^{pos}|\theta_{k-1}^{j})\right\}, \tag{8}$$

where $c_i(r_{i,k}^{pos}|\theta_{k-1}^{i,n})$ is the gas concentration estimated by the n_{th} particle of drone i at position $r_{i,k}^{pos}$, and $\sum_{j=1,j\neq i}^{N_r} c_j(r_{i,k}^{pos}|\theta_{k-1}^{j})$ represents the sum of gas concentration estimated by other particle filters at position $r_{i,k}^{pos}$.

We then utilize the Poisson observation model to determine the observation weight:

$$w_{obs}^{i,n}(r_{i,k}^{obs}, [r_{i,k}^{obs}]_{pred}) = \frac{[r_{i,k}^{obs}]_{pred}^{r_{i,k}^{obs}}\cdot\exp(-[r_{i,k}^{obs}]_{pred})}{(r_{i,k}^{obs})!}. \tag{9}$$

Through the application of the sequential importance sampling method [37], the iterative update of the estimation in Formula (5) is achieved by updating the corresponding weight, presented as:

Algorithm 1: Source term estimation based on parameter aggregation for drone i

Input : particle filter $\left\{\left(\theta_{k-1}^{i,n}, w_{k-1}^{i,n}\right)\right\}_{1\le n\le N_p}$; source term estimation θ_{k-1}^{j}, $j\in[1,N_r], j\neq i$; observed value $r_{i,k}^{obs}$

Output: particle filter $\left\{\left(\theta_{k}^{i,n}, w_{k}^{i,n}\right)\right\}_{1\le n\le N_p}$

for $n = 1 : N_p$ **do**
  Calculate the predicted value $[r_{i,k}^{obs}]_{pred}$ using Formula (8);
  Using observed value $r_{i,k}^{obs}$ and predicted value $[r_{i,k}^{obs}]_{pred}$ to calculate the observation weight $w_{obs}^{i,n}(r_{i,k}^{obs}, [r_{i,k}^{obs}]_{pred})$;
  Update the weight $\bar{w}_k^{i,n}$ based on the sequential importance sampling method;
end
Normalize the particle weights $w_k^{i,n} \leftarrow \bar{w}_k^{i,n}$;
Resample the particle based on roulette wheel selection;
Reset particle weights with uniform distribution;
Utilize the MCMC to increase the diversity of the particles;

$$\begin{cases} \bar{w}_k^{i,n} = w_{k-1}^{i,n} w_{obs}^{i,n}(r_{i,k}^{obs}, [r_{i,k}^{obs}]_{pred}) \\ w_k^{i,n} = \frac{\bar{w}_k^{i,n}}{\sum_{n=1}^{N_p} \bar{w}_k^{i,n}} \end{cases}. \tag{10}$$

To address the issue of rapid decay in particle weights caused by Formula (10) , we adopt a resampling step [19] to alleviate the particle degeneration phenomenon. Additionally, the Markov Chain Monte Carlo (MCMC) method [38] is also employed to increase the diversity of particles. The pseudocode of the source term estimation based on parameter aggregation is shown in Algorithm 1.

B. Cooperative mechanism based on dynamic likelihood weight

The source term estimation proposed in Section III-A may result in a single actual source being simultaneously estimated by multiple particle filters, preventing the drones from searching for additional unknown sources. To address this issue, a cooperative mechanism based on dynamic likelihood weight is introduced, which effectively facilitates the paired estimation and search between drones and unknown sources.

To alleviate the communication burden, we employ a Gaussian density function $\mathcal{N}(\cdot)$ to approximate the particle filter distribution P_k^i , expressed as:

$$P_k^i \approx \mathcal{N}\left(\mu_k^i, \Sigma_k^i\right), \tag{11}$$

where μ_k^i denotes the mean vector, and Σ_k^i denotes the covariance matrix. In the context of state estimation using a particle filter, these parameters equal the weighted sample mean and covariance of the particles $\left\{\left(\theta_k^{i,n}, w_k^{i,n}\right)\right\}_{1\le n\le N_p}$.

In multi-drone cooperative search scenarios, the Gaussian parameters shared among drones are utilized to quantify the dynamic likelihood weight β, which describes the possibility of a single drone accepting the estimation of the source term parameters from other drones. To prevent drones from simultaneously estimating the same actual source, the likelihood weight should be positively correlated with the difference in the probability distribution of source term estimation, defined as follows:

$$\beta_k^{ij} = \frac{1}{1+\exp(-D_{KL}(P_k^i||P_k^j))}, \tag{12}$$

where D_{KL} represents the Kullback-Leibler divergence, P_k^i and P_k^j are the posterior probability distributions of the estimated source term. Based on i_{th} drone's fitted Gaussian parameters $\{\mu_k^i, \Sigma_k^i\}$ and the shared Gaussian parameters $\{\mu_k^j, \Sigma_k^j\}$ from j_{th} drone, D_{KL} can be computed using the approximated expression [39]:

$$\begin{aligned} D\left(P_k^i \parallel P_k^j\right) \approx & \frac{1}{2}\Bigg\{ \log\frac{\left|\Sigma_k^j\right|}{\left|\Sigma_k^i\right|} - 2 + \operatorname{tr}\left(\left(\Sigma_k^j\right)^{-1}\Sigma_k^i\right) \\ & + \left(\mu_k^j - \mu_k^i\right)^{\mathrm{T}}\left(\Sigma_k^j\right)^{-1}\left(\mu_k^j - \mu_k^i\right)\Bigg\}. \end{aligned} \tag{13}$$

Algorithm 2: Cooperative mechanism based on dynamic likelihood weight for drone i

Input : multiple particle filters $\left\{\left(\theta_k^{i,n}, w_k^{i,n}\right)\right\}_{1\le n\le N_p}$, $i \in [1, N_r]$

Output: dynamic likelihood weight β_k^{ij}

```
Use the Gaussian density function N(·) to fit the distribution of the particle filter;
for j = 1 : N_r, j ≠ i do
    Compute the Kullback-Leibler divergence D(P_k^i ∥ P_k^j) based on the shared Gaussian parameters {μ_k^i, Σ_k^i} and {μ_k^j, Σ_k^j};
    Compute the likelihood weight β_k^ij using Formula (12);
end
```

From the two extreme cases in Formula (12), the following conclusions can be drawn: When the KL divergence is zero, the likelihood weight is 0.5, signifying a basic confidence level of 50%. This threshold prevents drones from conducting independent search without information sharing and collaboration. Conversely, as the KL divergence tends toward positive infinity, the likelihood weight asymptotically approaches 1, indicating that the drone i fully accepts the source term estimation provided by the drone j.

With the incorporation of the likelihood weight β, Formula (8) can be further formulated as follows:

$$\begin{aligned} [r_{i,k}^{obs}]_{pred} = 4\pi\sigma \cdot a\Bigg\{ & c_i(r_{i,k}^{pos}|\theta_{k-1}^{i,n}) \\ & + \sum_{j=1,j\neq i}^{N_r} \beta_{k-1}^{ij} c_j(r_{i,k}^{pos}|\theta_{k-1}^{j}) \Bigg\}. \end{aligned} \tag{14}$$

The β in Formula (14) enables one drone to disregard source term estimations from other drones that are similar to its own estimated state. This mechanism facilitates more accurate calculation of the predicted value at each step, thereby enhancing the drone's ability to estimate and search for unknown sources. The pseudocode of the cooperative mechanism based on dynamic likelihood weight is shown in Algorithm 2.

In the cognitive strategy, the reward function $F(u)$ is used to select the action u^* from the action set U with the highest information gain, given by $u^* = \arg\max\{F(u)\}_{u\in U}$. To achieve efficient search in multi-source scenarios, the Infotaxis II reward function [15] is utilized to control the behaviors of drones, formulated as:

$$\begin{aligned} F(u_k) = & -\int P\left(\hat{z}_{k+1}\middle|\theta_k^{i,n}\right) \\ & \times \int P\left(\theta_{k+1}^{i,n}\middle|\hat{z}_{k+1}, I_k^i\right)\log P\left(\theta_{k+1}^{i,n}\middle|\hat{z}_{k+1}, I_k^i\right) d\theta_k^{i,n} d\hat{z}_{k+1}, \end{aligned} \tag{15}$$

Algorithm 3: The application of the DLW-CI approach

Input : multiple particle filters $\left\{\left(\theta_{k=0}^{i,n}, w_{k=0}^{i,n}\right)\right\}_{1\le n\le N_p}$, $i \in [1, N_r]$; likelihood weight $\beta_{k=0}^{ij}$

Output: source term estimation θ_k^i

for $k = 1 : N_k$ **do**
  Collect observed value $r_{i,k}^{obs}$ for each drone at its position $r_{i,k}^{pos}$, with $i \in [1, N_r]$;
  for $i = 1 : N_r$ **do**
    for $n = 1 : N_p$ **do**
      Calculate the predicted value $[r_{i,k}^{obs}]_{pred}$ using Formula (14);
      Update the particle weight $\bar{w}_k^{i,n}$ based on the observed value $r_{i,k}^{obs}$ and predicted value $[r_{i,k}^{obs}]_{pred}$;
    end
    Normalize the particle weights $w_k^{i,n} \leftarrow \bar{w}_k^{i,n}$;
    Resample the particle based on roulette wheel selection;
    Reset particle weights with uniform distribution;
    Utilize the MCMC to increase the diversity of the particles;
  end
  Use the Gaussian density function $\mathcal{N}(\cdot)$ to fit the distribution of the particle;
  Compute the likelihood weight β_k^{ij} based on the shared Gaussian parameters;
  For each drone, choose the best action $u_{i,k}^* = \arg\max\{F(u)\}_{u\in U}$ and execute;
  if *meet the stopping condition* **then**
    Break;
  end
end

where $\hat{z}_{k+1}$ represents the expected observation at the next step. By utilizing the particle filter to approximate the source term estimation, Formula (15) is rewritten as follows:

$$F(u_k) \approx -\sum_{\hat{z}_{k+1}=0}^{N_z}\sum_{n=1}^{N_p} P(\hat{z}_{k+1}|\theta_k^{i,n})\hat{w}_{k+1}^{i,n}\log\hat{w}_{k+1}^{i,n}, \quad (16)$$

where $\hat{w}_{k+1}^{i,n}$ is the expected weight of the expected observation $\hat{z}_{k+1}$, and N_z denotes the maximum observation value that may be obtained.

The application of the DLW-CI approach is shown in Algorithm 3. The search continues until the global stopping criterion is satisfied. The task completion condition requires that all drones simultaneously meet two criteria: their estimated states must converge, meaning the particle filter variance falls below a specified threshold, and their estimated positions must be sufficiently close to the actual source locations. The source search task is considered successfully completed only when all drones meet both conditions. If the maximum allowed number of search steps is reached before the global stopping criterion is satisfied, the task is terminated and deemed unsuccessful.

C. Complexity analysis

The DLW-CI approach aggregates the information exchanged between drones to update the source term estimation, which guides the drones to take the most informative actions. As illustrated in Algorithm 3, the computational complexity of the DLW-CI approach primarily comprises three key components: the update of the particle filter, the calculation of the dynamic likelihood weight, and the optimization of the reward function. Specifically, in each iteration, their respective complexities are $O(N_r \times N_p \times m)$, $O(N_r^2 \times m^3)$, and $O(N_r \times |U| \times N_z \times N_p \times m)$, where m represents the dimension of the source parameters for a single source. Therefore, the total computational complexity O_T is given by:

$$\begin{aligned} O_T = {} & O(N_r \times N_p \times m) \\ & + O(N_r^2 \times m^3) + O(N_r \times |U| \times N_z \times N_p \times m). \end{aligned} \quad (17)$$

In terms of resource consumption, the cooperative mechanism requires each drone to broadcast its particle filter's Gaussian approximation parameters, consisting of the mean vector $\mu \in \mathbb{R}^m$ and covariance matrix $\Sigma \in \mathbb{R}^{m\times m}$. The symmetric nature of Σ reduces its transmission payload to the lower triangular components. The resulting communication load scales quadratically with state dimension m but remains linearly dependent on swarm size N_r, making the approach suitable for distributed platforms with limited bandwidth.

IV. Extensive Experiments

In this section, we demonstrate the overall performance and generalizability of the DLW-CI approach through a series of experiments. Section IV-A describes the experimental settings, involving dataset preparation, evaluation metrics, implementation details, and baseline methods. Section IV-B presents illustrative runs in both obstacle-free and obstacle-present scenarios to detail the typical source search process. To highlight the advantages of DLW-CI, we compare it with baseline methods in Section IV-C within obstacle-free environments. Additionally, Section IV-D examines how key parameters affect the robustness and reliability of DLW-CI. Finally, in Section IV-E, we utilize the computational fluid dynamics (CFD) software, FLUENT, to generate a gas diffusion field as the ground truth, and conduct a case study to further validate our proposed approach.

A. Experimental settings

1) Dataset preparation : To evaluate the performance of DLW-CI, we create multi-source diffusion scenarios using a convection-diffusion model. The simulation takes place in a $10m \times 10m$ square area with $N_s = 3$ diffusion sources randomly distributed. Environment, drones, and particle filter parameters are listed in Table I. Unless stated otherwise, the default values are used for all experiments in this paper.

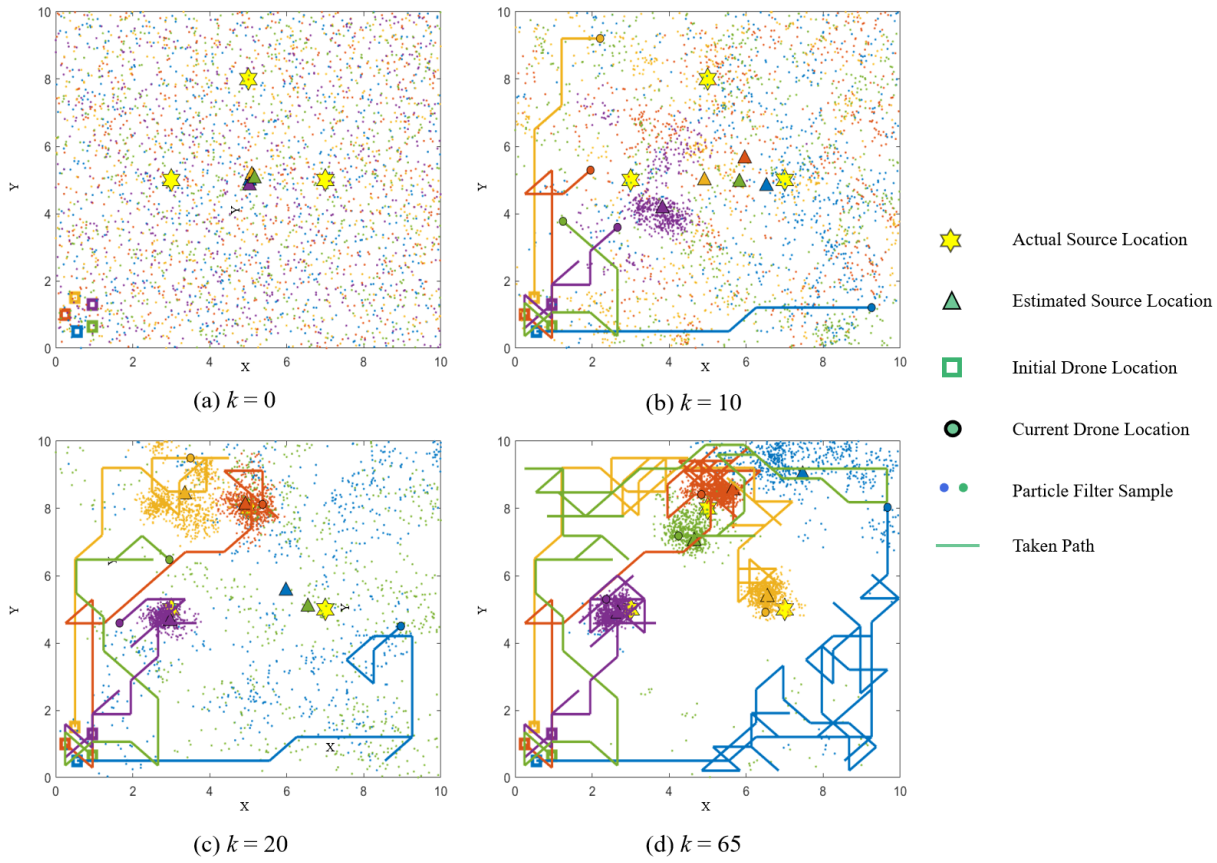

Fig. 5. An illustrative run of the DLW-CI approach in an obstacle-free scenario at different time steps: (a) k= 0, (b) k= 10, (c) k= 20, (d) k= 65.

TABLE I
EXPERIMENTAL PARAMETER CONFIGURATIONS

	Parameter	Value
Environment	Search domain $\mathcal{D}$	$10m \times 10m$
	Number of sources N_s	3
	Wind speed v	1
	Wind direction ϕ_v	90°
	Coefficient of diffusion σ	1
	Gas molecular lifetime τ	250
	Diffusion strength s^{str}	3
Drone	Size of drone a	1
	Number of drones N_r	5
	Step length r_{step}	1
	Maximum observed value N_z	7
	Optional action set U	$\{\uparrow, \nearrow, \rightarrow, \searrow, \downarrow, \swarrow, \leftarrow, \nwarrow\}$
Particle filter	Number of particles N_p	700
	Source x-position	$\mathbb{U}(0, 10)$
	Source y-position	$\mathbb{U}(0, 10)$
	Source release strength	$\mathbb{U}(0, 4)$

2) Evaluation metrics: The performance of the proposed approach is evaluated using three primary metrics: Success Rate (SR), Accuracy, and Root Mean Square Error (RMSE). SR measures the frequency with which the drones successfully locate all unknown sources within the specified criteria. Accuracy reflects the drones' ability to correctly identify source locations. RMSE quantifies the discrepancy between the estimated and actual source positions. A search is considered successful if the particle filter variance for each drone converges below 1 and the Euclidean distance between the estimated and actual source positions is less than 1 unit. If these criteria are not met within the maximum of $N_k = 100$ search steps, the task is marked as unsuccessful. Together, these metrics provide a comprehensive assessment of the algorithm's efficiency, accuracy, and robustness in multi-source localization tasks.

3) Implementation details: All simulations in Section IV were performed using Matlab R2023b on a system equipped with an AMD Ryzen 9 7945HX 2.50 GHz CPU and an NVIDIA GeForce RTX 4060 Laptop GPU.

4) Baseline methods : The DLW-CI approach is compared against niching PSO and Infotaxis. Niching PSO, a multi-robot collaborative search strategy specifically designed for multi-source localization, is chosen as a baseline due to its capability in addressing the local optima problem inherent in multi-source environments. Infotaxis, a classic cognitive strategy typically employed in single-source scenarios, is included to evaluate the effectiveness of directly applying a cognitive strategy to more complex multi-source problems, thereby highlighting the advantages of the proposed DLW-CI approach. Besides, the performance of DLW-CI without the likelihood weight is also compared. Concentration field fitting methods are excluded from the comparison, as their primary objective of fitting a concentration field similar to the actual

scene differs fundamentally from the tasks of our research.

B. Illustrative run

Here we respectively present the illustrative run of DLW-CI in an obstacle-free scenario and an obstructed scenario.

1) Illustrative run in an obstacle-free scenario: The illustrative run in an obstacle-free scenario is configured with the following parameters, as shown in Table I. In the $10m \times 10m$ square area, three diffusion sources are respectively located at $\{(3,5),(5,8),(7,5)\}$, while five drones are located at the left bottom of the scenario.

As shown in Fig. 5, the yellow polygon marks the actual position of the source, while the black-edged triangle indicates the estimated source location. The square represents the drone's starting point, and the black-edged circle shows its current position. Colored dots correspond to samples from different particle filters. The drone's trajectory is shown as a straight line. To illustrate the pairing between each drone and its corresponding source, the colors of the drone's position, estimated source location, particle filter samples, and trajectory are matched.

In Fig. 5, at step $k = 0$, the initial state of the source search process, the samples of each particle filter are uniformly distributed across the multi-source scenario. The DLW-CI approach guides the drones to perform a paired source search task by aggregating the estimation of the source term from the drones. At step $k = 10$, the purple particles gradually converge toward the source located in the lower-left corner of the scene. At step $k = 20$, the purple and orange particles have respectively aggregated near the lower-left and upper sources. Finally, at step $k = 65$, the purple, orange, and yellow particles have gathered near the three source locations, satisfying the termination condition for the source search task.

In Fig. 5(d), the green and orange particles converging at both ends of the upper source indicate that the two drones' estimates closely match the actual concentration distribution. Table II further comfirms this, showing that the sum of the estimated source strengths from the two drones equals the actual upper source strength. Meanwhile, the blue particles in the upper right corner suggest the possibility of an unknown source. However, Table II shows that the blue drone's estimated source strength is zero, smeaning the blue drone correctly identifies that no source exists in that area. These results support the effectiveness of our proposed paired estimation and search strategy between drones and sources.

Fig. 6(a) shows how the orange drone's likelihood weight toward other drones changes over time. The orange drone maintains a baseline likelihood weight of 0.5, ensuring its ongoing collaboration. During the interval $[0, 10]$, its likelihood weight toward the purple drone increases sharply. Concurrently, Fig. 5(b) shows purple particles converging near the lower-left source, while orange particles remain dispersed—indicating the purple drone has found its source location. In the interval $[10, 20]$, the orange drone's likelihood weight toward other drones increases to 1, with orange particles converging in Fig. 5(c), showing the orange drone has identified its own source. This dynamic adjustment of likelihood weights between drones significantly improves collaboration and ensures accurate source estimation.

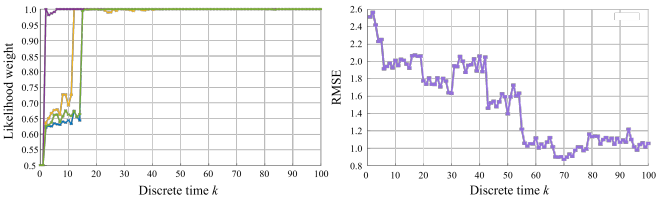

(a) Dynamic change of the likelihood weight (b) Variation of the RMSE

Fig. 6. Numerical variations during the source search. (**a**) The dynamic change of the orange drone's likelihood weight to other drones; (**b**) The variation of the RMSE between the estimated and the actual source location.

TABLE II
SOURCE TERM ESTIMATED BY EACH DRONE AT THE END OF THE SOURCE SEARCH TASK

Drone Color	x-coordinate	y-coordinate	Source strength
Blue	7.1137	9.0088	0
Green	4.8093	7.2918	1
Orange	5.7466	8.4518	2
Purple	2.8513	4.8811	3
Yellow	6.5718	5.2832	3

2) Illustrative run in an obstructed scenario: In the obstructed scenario, the illustrative run is conducted within a $20m \times 20m$ square area with three sources respectively located at $\{(5,10),(10,15),(15,10)\}$. The drones are initially deployed at the bottom of the scenario, with an optional action set $U = \{\uparrow, \rightarrow, \downarrow, \leftarrow\}$ and step length $r_{step} = 0.5$. The initial particle filter's location distribution follows a uniform distribution $\mathbb{U}(0, 20)$, with the number of particles set to $N_p = 2000$. Due to the enlargement of the scenario and the reduction of the drone step length, the maximum number of search steps is adjusted to $N_k = 500$. Apart from the parameter settings mentioned above, all other experimental parameters use the default values listed in Table I. The source search process is shown in Fig. 7.

In Fig. 7, at step $k = 0$, the multiple particle filters are uniformly distributed in the source search scenario. At step $k = 50$, the yellow particles cluster around the lower-left source. At step $k = 145$, the blue particles converge toward the lower-right source. Finally, at step $k = 225$, the purple particles aggregate near the upper source. For each actual source location, a corresponding estimated source location emerges, with associated particle filters converging. This convergence indicates the successful completion of the source search task. These results demonstrate that even in an obstacle environment with significant spatial barriers, the DLW-CI approach can also enable drones to complete the multi-source search task.

C. Performance comparisons with baselines

In this section, we conduct comprehensive simulation experiments in obstacle-free scenarios to evaluate and compare the performance of the DLW-CI approach against baseline methods. Baseline methods are described in Section IV-A4.

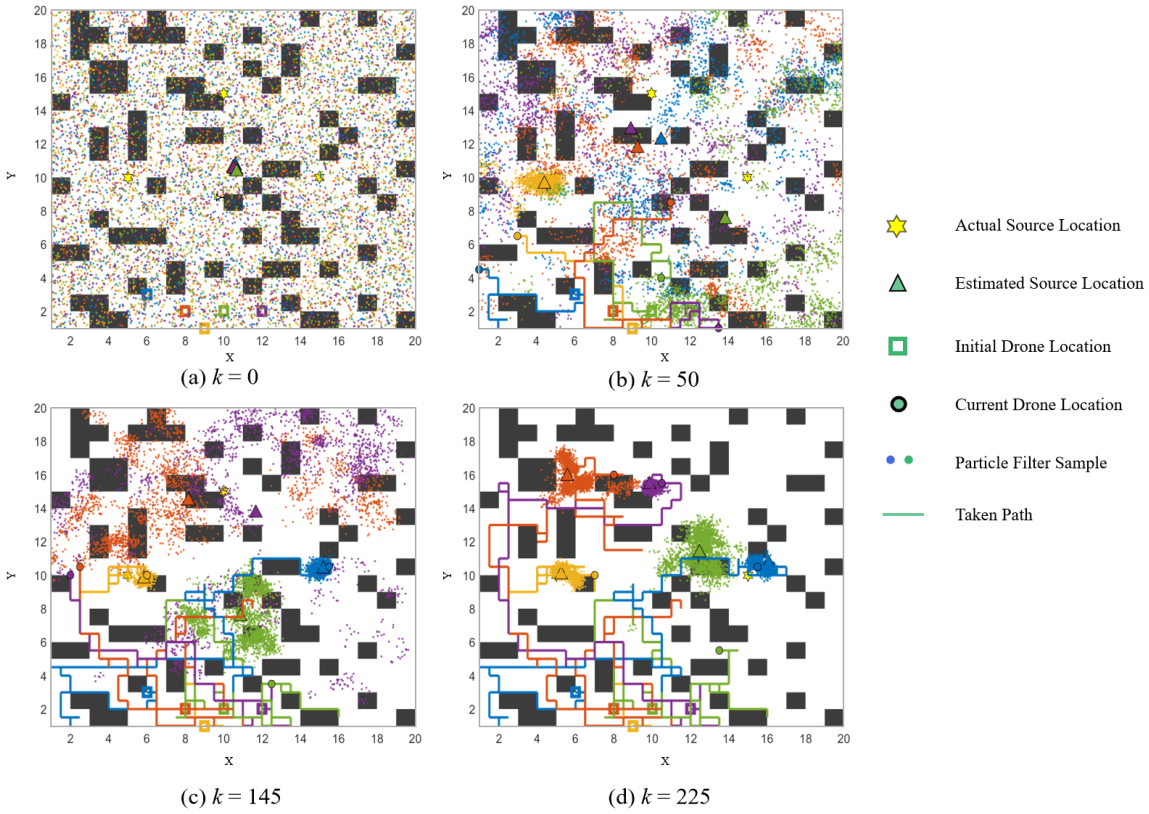

(a) $k = 0$ (b) $k = 50$ (c) $k = 145$ (d) $k = 225$

Fig. 7. An illustrative run of the DLW-CI approach in an obstacle scenario at different time steps: (a) k= 0, (b) k= 50, (c) k= 145, (d) k= 225.

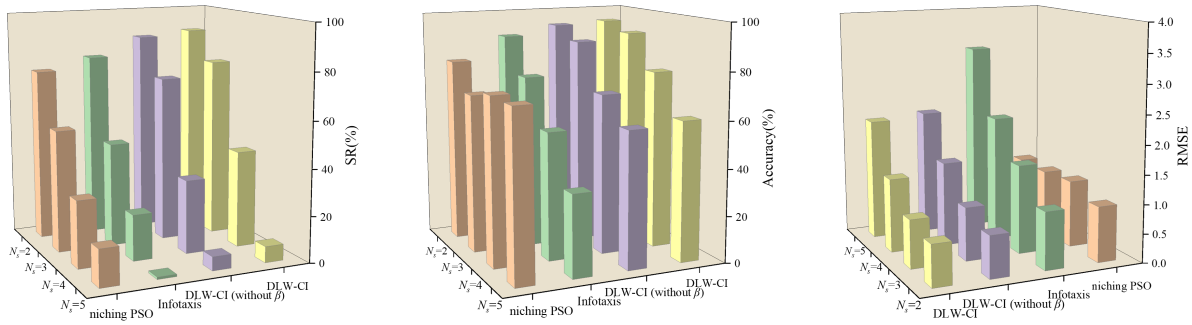

(a) Success Rate (b) Accuracy (c) Root Mean Square Error

Fig. 8. Performance comparison between the DLW-CI approach and baselines in the different obstacle-free scenarios ($N_s = \{2, 3, 4, 5\}$).

The simulation parameters follow the settings in Table I, with the exception of the independent variables. The experimental scenarios have four different multi-source settings with varying numbers of sources $N_s = \{2, 3, 4, 5\}$. Each setting consists of 100 maps, with the locations of the sources and drones being randomly generated.

Fig. 8 shows the experimental results in obstacle-free scenarios. In multi-source scenarios with unknown source counts $N_s = \{2, 3\}$, the DLW-CI approach outperforms both the niching PSO algorithm and the Infotaxis cognitive search strategy in terms of success rate, accuracy, and RMSE. Additionally, incorporating the likelihood weight β further enhances the algorithm's performance, leading to improved results.

However, when the number of unknown sources increases to $N_s = \{4, 5\}$, the effectiveness of the proposed approach decreases. As illusrated in Fig. 8(b), the average number of accurately located sources is about 3 when $N_s \geq 3$. This limitation likely arises because the aggregated estimated states cannot fully capture the complexity of multiple sources. In summary, compared to the baselines, the DLW-CI approach demonstrates enhanced performance in scenarios with fewer sources, providing more accurate source localization and stable

TABLE III
THE SEARCH PERFORMANCE OF DLW-CI UNDER DIFFERENT COMBINATIONS OF SOURCE STRENGTH s^{str} AND WIND SPEED v.

Measure	(s^{str}, v)	$v=0$	$v=1$	$v=2$
SR (%)	$s^{str}=2$	57	64	62
	$s^{str}=3$	62	78	76
	$s^{str}=4$	55	80	77
Accuracy (%)	$s^{str}=2$	79.33	83.67	84.33
	$s^{str}=3$	79.67	91.00	89.00
	$s^{str}=4$	74.67	92.33	90.67
RMSE	$s^{str}=2$	1.2036	1.0077	1.0593
	$s^{str}=3$	1.0382	0.8408	0.8416
	$s^{str}=4$	0.9869	0.8133	0.8690

TABLE IV
THE SEARCH PERFORMANCE OF DLW-CI UNDER DIFFERENT COMBINATIONS OF DRONE NUMBER N_r AND SOURCE NUMBER N_s.

Measure	(N_r, N_s)	$N_s=2$	$N_s=3$	$N_s=4$	$N_s=5$
SR (%)	$N_r=5$	90	78	42	7
	$N_r=6$	91	81	54	24
	$N_r=7$	98	84	64	51
Accuracy (%)	$N_r=5$	94.50	91.00	76.75	60.00
	$N_r=6$	94.50	93.00	82.50	65.20
	$N_r=7$	99.00	94.67	90.00	80.00
RMSE	$N_r=5$	0.7171	0.8416	1.2865	2.1108
	$N_r=6$	0.5860	0.6496	1.0561	1.6081
	$N_r=7$	0.5408	0.6171	0.8162	0.9449

search capability.

These results are obtained in obstacle-free scenarios, whereas obstacles are prevalent in real urban environments. The baseline methods perform poorly or even fail in the presence of obstacles, while DLW-CI proposed in this paper maintains a certain level of search success rate and estimation accuracy. Detailed results are provided in case study.

D. Hyper-parameter experiments

In this section, we evaluate the robustness of DLW-CI in obstacle-free scenarios. First, we test its effectiveness under varying source strengths and wind speeds. Next, we examine how the number of drones and unknown sources affects performance. Finally, we analyze the influence of the number of particles in the particle filter on the results. Except for the independent variables, all simulation parameters strictly followed the settings in Table I.

1) Source strength and wind speed: In single-source scenarios, previous studies have demonstrated that the source strength s^{str} and wind speed v can impact algorithm performance. To investigate whether these factors similarly affect algorithm performance in multi-source scenarios, Monte Carlo simulations are conducted under varying source strengths and wind speeds, with each group of simulations executed 100 times. In each simulation, the source locations and the initial positions of the drones are randomly generated.

The experimental results under various environmental conditions are summarized in Table III, revealing three main trends: (1) For a fixed source strength, performance improves with increasing wind speed up to a point, then declines. For example, at $s^{str}=3$, the SR rises from 62% at $v=0$ to 78% at $v=1$, before dropping to 76% at $v=2$. (2) In windless conditions ($v=0$), the optimal performance is achieved at $s^{str}=3$, with an SR of 62%, an accuracy of 79.67%, and RMSE of 1.0382. Performance decreases at higher source strengths; for instance, at $s^{str}=4$, the SR falls to 55% and accuracy to 74.67%. (3) Under wind conditions ($v=1,2$), stronger source stengths consistently yield better results. At $v=1$, the SR increases from 64% at $s^{str}=2$ to 80% at $s^{str}=4$, while the RMSE decreases from 1.0077 to 0.8133. These results demonstrate that DLW-CI is robust, particularly under moderate wind and strong source strength conditions.

2) Quantity between drones and sources: The proposed approach in this study is based on the assumption that the number of drones N_r is no less than the number of unknown sources N_s. To test the validity of the hypothesis, Monte Carlo experiments are conducted to investigate the effect of N_r and N_s on the performance of the DLW-CI approach, with results presented in Table IV. We can observe that when the number of drones is held constant (e.g. $N_r=5$), an increase in the number of leakage sources from 2 to 5 leads to a pronounced decline in SR from 90% to 7%, a decrease in accuracy from 94.5% to 60.0%, and an increase in RMSE from 0.7171 to 2.1108. The finding indicates that the algorithm's adaptability to multi-source scenarios is significantly constrained when drone numbers are limited.

Notably, when the difference between the number of drones and the number of sources $N_r - N_s \geq 2$, the algorithm's performance is remarkably enhanced. For instance, when $N_s=3$, increasing N_r from 5 to 7 raises the SR from 78% to 84%. Similarly, for the scenario with $N_s=5$, the SR of 51% when $N_r=7$ is nearly seven times higher than that when $N_r=5$ (7%). These results underscore the critical role of drone redundancy in improving the algorithm's performance for multi-source search tasks. We recommend that, in practical deployments, the number of drones should be at least $N_r \geq N_s+2$ to ensure effective collaborative search capabilities. Additionally, the results show that in complex scenarios ($N_s \geq 4$), the algorithm tends to reliably identify approximately three sources, with an average accuracy ranging from 76.8% to 90.0%. This phenomenon may be related to the aggregation mechanism of the particle filter and warrants further investigation in future studies.

3) Sample number in the particle filter: In this study, the source term estimation is approximated by the particle filter, which is significantly influenced by the number of particles N_p. This section investigates the impact of N_p on the search performance of the DLW-CI approach. Each group of simulations is executed 100 times, and the experimental results are presented in Table V. It is observed that the results reveal a distinct nonlinear relationship between particle number and algorithm performance. Specifically, as N_p increases from 200 to 650, the SR rises significantly from 54% to 84%, accuracy increases from 80.00% to 93.67%, and RMSE decreases from 1.1388 to 0.6779. These improvements highlight the

TABLE V
THE SEARCH PERFORMANCE OF DLW-CI APPROACH UNDER DIFFERENT SAMPLE NUMBER N_p

Measure	200	350	500	650	800	950
SR (%)	54	78	80	**84**	78	80
Accuracy (%)	80.00	91.00	92.00	**93.67**	90.85	91.33
RMSE	1.1388	0.8416	0.8012	**0.6779**	0.7723	0.6807

positive impact of increasing particle number on algorithm performance.

However, when N_p exceeds 650, further increases in particle number lead to a decline in performance. For example, at $N_p = 800$, the SR drops to 78%, and the RMSE rises to 0.7723. This phenomenon indicates that there is an optimal interval for particle number (around $N_p = 650$), where the algorithm achieves a balance between computational cost and search accuracy.

Notably, the performance metrics for $N_p = 650$ (SR $= 84\%$, accuracy $= 93.67\%$, RMSE $= 0.6779$) are comprehensively superior to other configurations. This finding underscores the importance of selecting an appropriate particle number to maintain the estimation accuracy of the particle filter. Based on these results, we recommend setting the number of particles in the range of 600–700 in practice. This range ensures sufficient space coverage while avoiding estimation drift caused by an excessive number of particles.

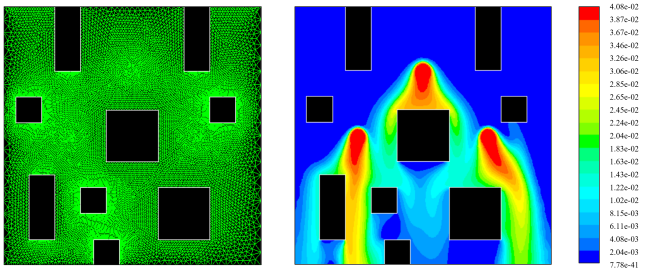

(a) Obstacle map constructed by GAMBIT (b) Methane diffusion simulated by FLUENT

Fig. 9. Diffusion affected by obstacles scenario constructed: (a) A triangular grid map built by Gambit; (b) The multi-source diffusion scenario generated based on the CFD model.

E. Case study

In this section, we employ the CFD model to generate a realistic concentration field and examine the applicability of our approach in scenarios where gas diffusion is influenced by obstacles. Following previous studies [40], [41], [42], we utilize GAMBIT to generate and mesh obstacle scenarioa depicted in Fig. 9(a). The concentration data predicted by FLUENT is then used to replace the data from the convective diffusion model for experimental validation.

The diffusion field generated by FLUENT is shown in Fig. 9(b). The black wall simultaneously influences both the leakage source diffusion and drone movements. A steady wind flows from the upper window, while pressure outlets are configured on the remaining three boundary windows. Three sources continuously release methane (CH_4) into the environment. The concentration visualization employs a brightness gradient, with brighter regions indicating higher CH_4 concentrations. The red zones represent the highest concentration points, precisely aligning with the actual source locations.

In this simulation, a network of five consumer drones is deployed to explore the $20m \times 20m$ search domain and identify the leakage sources. The sources are respectively positioned at $\{(5, 10), (10, 15), (15, 10)\}$, emitting chemicals at a release rate of $100kg/m^2 \cdot s$. The k-epsilon turbulence model is used to simulate turbulent effects, with turbulence intensity and viscosity in the scene set to 10% and 10 respectively. The wind speed is set to $1m/s$. The consumer drones initiate their search from the left-bottom corner of the scenario, choosing actions from the action set $U = \{\uparrow, \rightarrow, \downarrow, \leftarrow\}$ and adopting a step length of $r_{step} = 0.5$. The initial locations of particles in the particle filter follow a uniform distribution $\mathbb{U}(0, 20)$, and source release strengths are distributed according to $\mathbb{U}(0, 4)$. The particle filter comprises $N_p = 2000$ particles. The source search process in the obstacle-affected gas diffusion scenario is illustrated in Fig. 10. At step $k = 0$, multiple particle filters are uniformly distributed within the search scene. At step $k = 45$, the orange particles cluster around the lower-left source. At step $k = 185$, the purple particles converge toward the upper source. Finally, at step $k = 205$, the yellow particles aggregate near the lower-right source. As shown in the figure, the proposed DLW-CI approach effectively overcomes local optimum constraints when guiding drone actions, enabling more thorough exploration of unknown sources.

V. DISCUSSION AND CONCLUSION

In this study, we proposed the DLW-CI approach to address the challenges of multi-source search in hazardous substance leakage scenarios using consumer-grade drone networks as AISs. Our approach integrates the cognitive strategy of infotaxis with a novel cooperative mechanism based on dynamic likelihood weight, enabling multiple consumer drones to efficiently and accurately locate unknown sources in complex environments with minimal computational and energy resources. The main contributions of this work include developing a multi-drone collaborative source estimation approach utilizing parallel particle filters and introducing a dynamic likelihood-weighted cooperative mechanism that prevents redundant source estimation while improving search coverage.

Our experimental results show that the DLW-CI approach outperforms the niching PSO algorithm in scenarios with 2, 3, and 4 diffusion sources, achieving a 37.33% improvement in success rate, a 19.55% increase in accuracy, and a 12.59% reduction in RMSE on average. The dynamic likelihood-weighted cooperative mechanism enhances the pairing between consumer drones and unknown sources, resulting in more precise source localization. However, the algorithm's performance declines as the number of unknown sources increases, highlighting its limitations in handling highly complex multi-source scenarios with consumer-grade hardware. The robustness of the DLW-CI approach is further validated through extensive experiments under varying conditions, including

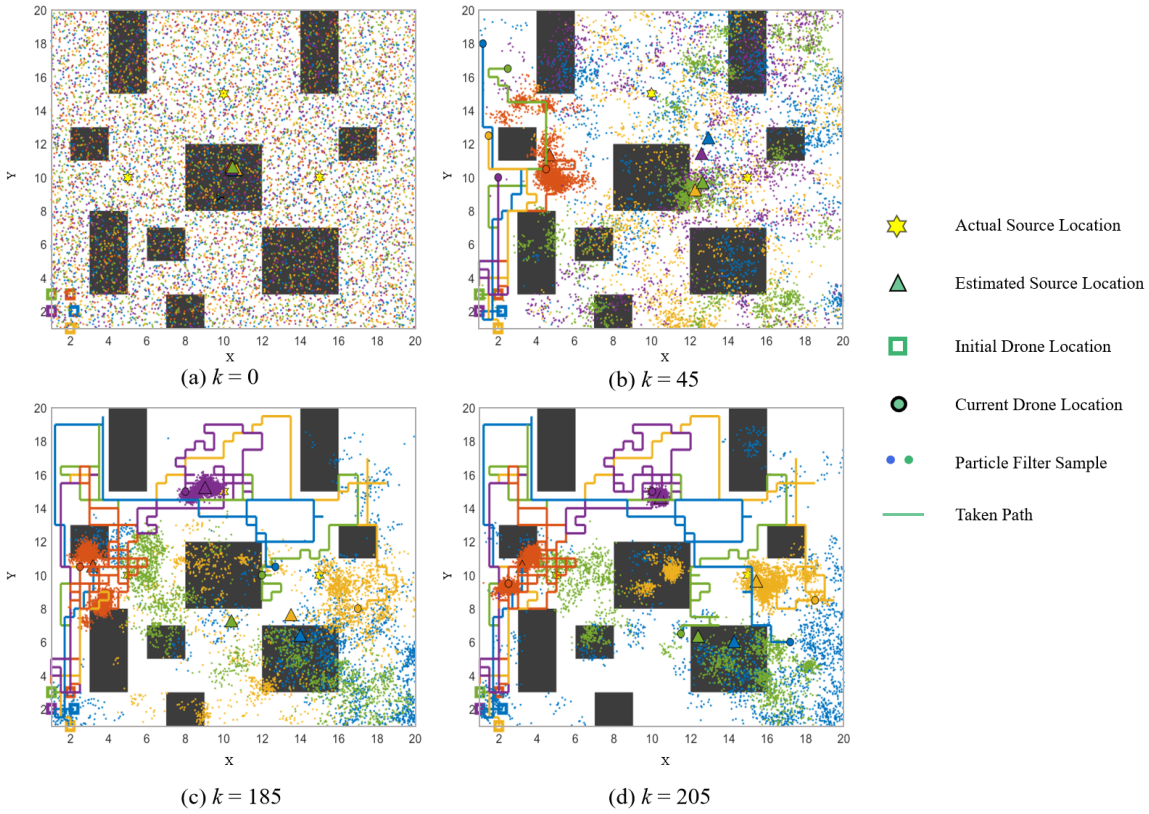

Fig. 10. The source search process in a diffusion scenario based on the CFD model at different time steps: (a) k= 0, (b) k= 45, (c) k= 185, (d) k= 205.

different source strengths, wind speeds, numbers of drones and sources, and particle filter sizes. The results indicate that the algorithm performs best when the number of drones exceeds the number of sources by at least two and when the number of particles is optimally balanced to prevent under- or over-sampling, providing practical deployment guidelines for consumer AIS implementations. The applicability of DLW-CI to real-world urban scenarios is further evaluated through a case study based on the CFD model.

In conclusion, the DLW-CI approach represents a significant advancement in multi-drone cooperative multi-source search, offering a novel solution for hazardous substance localization using consumer drones in city environments. By enabling affordable, energy-efficient detection systems, this research contributes to environmental safety monitoring and urban health protection. Future work will focus on enhancing the DLW-CI approach's scalability to handle more complex multi-source scenarios while maintaining computational efficiency for consumer hardware. Additionally, we aim to develop adaptive mechanisms for dynamically switching between multi-source and single-source search modes, depending on the real-time characteristics of the concentration field. Moreover, we will validate these improvements in real scenarios to test the robustness and validity of the proposed approach.

REFERENCES

[1] S. A. Nooh, "Optimizing low carbon sustainable environmental monitoring with consumer technology: An iot-driven federated learning approach for edge computing optimization," *IEEE Trans. Consum. Electron.*, pp. 1–1, 2025.

[2] J. Akram, A. Anaissi, R. S. Rathore, R. H. Jhaveri, and A. Akram, "Galtrust: Generative adverserial learning-based framework for trust management in spatial crowdsourcing drone services," *IEEE Trans. Consum. Electron.*, 2024.

[3] Z. Li, W.-H. Chen, and C. Liu, "Review of uav-based autonomous search algorithms for hazardous sources," *SCIENTIA SINICA Informationis*, vol. 52, no. 9, pp. 1579–1597, 2022.

[4] Y. Zhao, B. Chen, Z. Zhu, F. Chen, Y. Wang, and Y. Ji, "Searching the diffusive source in an unknown obstructed environment by cognitive strategies with forbidden areas," *Build. Environ.*, vol. 186, p. 107349, 2020.

[5] A. Mukherjee, D. De, N. Dey, R. G. Crespo, and E. Herrera-Viedma, "Disastdrone: A disaster aware consumer internet of drone things system in ultra-low latent 6g network," *IEEE Trans. Consum. Electron.*, vol. 69, no. 1, pp. 38–48, 2022.

[6] G. Suchanek, J. Wołoszyn, and A. Gołaś, "Evaluation of selected algorithms for air pollution source localisation using drones," *Sustainability*, vol. 14, no. 5, p. 3049, 2022.

[7] Y.-H. Ho and Y.-J. Tsai, "Open collaborative platform for multi-drones to support search and rescue operations," *Drones*, vol. 6, no. 5, p. 132, 2022.

[8] X.-x. Chen and J. Huang, "Odor source localization algorithms on mobile robots: A review and future outlook," *Robot. Auton. Syst.*, vol. 112, pp. 123–136, 2019.

[9] A. Francis, S. Li, C. Griffiths, and J. Sienz, "Gas source localization and mapping with mobile robots: A review," *J. FIELD. ROBOT.*, vol. 39, no. 8, pp. 1341–1373, 2022.

[10] M. Hutchinson, H. Oh, and W.-H. Chen, "A review of source term estimation methods for atmospheric dispersion events using static or mobile sensors," *Inform. Fusion.*, vol. 36, pp. 130–148, 2017.

[11] R. Guo, Y. Zhao, Y. Ji, M. Yan, and Z. Zhu, "Clutaxis: an information-driven source search method balancing exploration and exploitation in turbulent environments," *J. Saf. Sci. Resil.*, 2024.

[12] F. W. Grasso, J. A. Basil, and J. Atema, "Toward the convergence: robot and lobster perspectives of tracking odors to their source in the

turbulent marine environment," in *Proc. IEEE Int. Symp. Intell. Control (ISIC) held jointly with IEEE Int. Symp. Comput. Intell. Robot. Automat. (CIRA)*. IEEE, 1998, pp. 259–264.

[13] Y. Kuwana, S. Nagasawa, I. Shimoyama, and R. Kanzaki, "Synthesis of the pheromone-oriented behaviour of silkworm moths by a mobile robot with moth antennae as pheromone sensors," *Biosens. Bioelectron.*, vol. 14, no. 2, pp. 195–202, 1999.

[14] H. Ishida, K.-i. Suetsugu, T. Nakamoto, and T. Moriizumi, "Study of autonomous mobile sensing system for localization of odor source using gas sensors and anemometric sensors," *Sensor. Actuat. A-Phys.*, vol. 45, no. 2, pp. 153–157, 1994.

[15] B. Ristic, A. Skvortsov, and A. Gunatilaka, "A study of cognitive strategies for an autonomous search," *Inform. Fusion.*, vol. 28, pp. 1–9, 2016.

[16] Y. Ji, Y. Zhao, B. Chen, Z. Zhu, Y. Liu, H. Zhu, and S. Qiu, "Source searching in unknown obstructed environments through source estimation, target determination, and path planning," *Build. Environ.*, vol. 221, p. 109266, 2022.

[17] Y. Zhao, B. Chen, Z. Zhu, F. Chen, Y. Wang, and D. Ma, "Entrotaxis-jump as a hybrid search algorithm for seeking an unknown emission source in a large-scale area with road network constraint," *Expert. Syst. Appl.*, vol. 157, p. 113484, 2020.

[18] M. Vergassola, E. Villermaux, and B. I. Shraiman, "'infotaxis' as a strategy for searching without gradients," *Nature*, vol. 445, no. 7126, pp. 406–409, 2007.

[19] M. Hutchinson, H. Oh, and W.-H. Chen, "Entrotaxis as a strategy for autonomous search and source reconstruction in turbulent conditions," *Inform. Fusion.*, vol. 42, pp. 179–189, 2018.

[20] C. Song, Y. He, B. Ristic, and X. Lei, "Collaborative infotaxis: Searching for a signal-emitting source based on particle filter and gaussian fitting," *Robot. Auton. Syst.*, vol. 125, p. 103414, 2020.

[21] Y. Ji, F. Chen, B. Chen, Y. Wang, X. Zhu, and H. He, "Multi-robot collaborative source searching strategy in large-scale chemical clusters," *IEEE Sens. J.*, vol. 22, no. 18, pp. 17 655–17 665, 2021.

[22] I. Farhat, W. Hamidouche, A. Grill, D. Ménard, and O. Déforges, "Lightweight hardware transform design for the versatile video coding 4k asic decoders," *IEEE Trans. Consum. Electron.*, vol. 67, no. 4, pp. 329–340, 2021.

[23] G. Cabrita, L. Marques, and V. Gazi, "Virtual cancelation plume for multiple odor source localization," in *Proc. IEEE/RSJ Int. Conf. Intell. Robots Syst. (IROS)*. IEEE, 2013, pp. 5552–5558.

[24] J. Zhang, D. Gong, and Y. Zhang, "A niching pso-based multi-robot cooperation method for localizing odor sources," *Neurocomputing*, vol. 123, pp. 308–317, 2014.

[25] Y. Zou and D. Luo, "A modified ant colony algorithm used for multi-robot odor source localization," in *Proc. Int. Conf. Intell. Comput. (ICIC)*. Springer, 2008, pp. 502–509.

[26] U. Jain, R. Tiwari, and W. W. Godfrey, "Multiple odor source localization using diverse-pso and group-based strategies in an unknown environment," *J. Comput. Sci.*, vol. 34, pp. 33–47, 2019.

[27] Y. Ji, Y. Zhao, B. Chen, H. Zhu, Z. Zhu, S. Qiu, and Q. Yin, "A role-based informative source search approach for indoor multiple sources localization," *Available at SSRN 4757227*, 2024.

[28] A. S. Leong and M. Zamani, "Field estimation using binary measurements," *Signal. Process.*, vol. 194, p. 108430, 2022.

[29] V. P. Tran, M. A. Garratt, K. Kasmarik, S. G. Anavatti, A. S. Leong, and M. Zamani, "Multi-gas source localization and mapping by flocking robots," *Inform. Fusion.*, vol. 91, pp. 665–680, 2023.

[30] M. Stynes, "Steady-state convection-diffusion problems," *Acta Numer.*, vol. 14, pp. 445–508, 2005.

[31] S. Liu, M. Watterson, K. Mohta, K. Sun, S. Bhattacharya, C. J. Taylor, and V. Kumar, "Planning dynamically feasible trajectories for quadrotors using safe flight corridors in 3-d complex environments," *IEEE Rob. Autom. Lett.*, vol. 2, no. 3, pp. 1688–1695, 2017.

[32] A. Bircher, M. Kamel, K. Alexis, H. Oleynikova, and R. Siegwart, "Receding horizon "next-best-view" planner for 3d exploration," in *Proc. IEEE Int. Conf. Robot. Autom. (ICRA)*, 2016, pp. 1462–1468.

[33] H. C. Berg and E. M. Purcell, "Physics of chemoreception," *Biophys. J.*, vol. 20, no. 2, pp. 193–219, 1977.

[34] M. v. Smoluchowski, "Versuch einer mathematischen theorie der koagulationskinetik kolloider lösungen," *Zeitschrift für physikalische Chemie*, vol. 92, no. 1, pp. 129–168, 1918.

[35] E. K. Chong, C. M. Kreucher, and A. O. Hero III, "Pomdp approximation using simulation and heuristics," in *Foundations and applications of sensor management*. Springer, 2008, pp. 95–119.

[36] M. S. Arulampalam, S. Maskell, N. Gordon, and T. Clapp, "A tutorial on particle filters for online nonlinear/non-gaussian bayesian tracking," *IEEE Trans. Signal Process.*, vol. 50, no. 2, pp. 174–188, 2002.

[37] B. Ristic, S. Arulampalam, and N. Gordon, *Beyond the Kalman filter: Particle filters for tracking applications*. Artech house, 2003.

[38] N. Chopin, "A sequential particle filter method for static models," *Biometrika*, vol. 89, no. 3, pp. 539–552, 2002.

[39] J.-L. Durrieu, J.-P. Thiran, and F. Kelly, "Lower and upper bounds for approximation of the kullback-leibler divergence between gaussian mixture models," in *Proc. IEEE Int. Conf. Acoust., Speech Signal Process. (ICASSP)*. IEEE, 2012, pp. 4833–4836.

[40] F. Xue, X. Li, R. Ooka, H. Kikumoto, and W. Zhang, "Turbulent schmidt number for source term estimation using bayesian inference," *Build. Environ.*, vol. 125, pp. 414–422, 2017.

[41] G. C. Efthimiou, I. V. Kovalets, C. D. Argyropoulos, A. Venetsanos, S. Andronopoulos, and K. E. Kakosimos, "Evaluation of an inverse modelling methodology for the prediction of a stationary point pollutant source in complex urban environments," *Build. Environ.*, vol. 143, pp. 107–119, 2018.

[42] M. Awadalla, T.-F. Lu, Z. F. Tian, B. Dally, and Z. Liu, "3d framework combining cfd and matlab techniques for plume source localization research," *Build. Environ.*, vol. 70, pp. 10–19, 2013.

ABOUT THE AUTHOR

Xiaoran Zhang received the B.E. degree in simulation engineering from National University of Defense Technology, Changsha, China, in 2024, where he is currently pursuing the master degree in control science and engineering. His research interests include consumer drones and computer vision.

Yatai Ji received the M.E. degree in control science and engineering from the National University of Defense Technology, Changsha, China, in 2022, where he is currently working toward the Ph.D. degree in control science and engineering. His research focuses on source search and deep learning.

Yong Zhao received the M.E. degree in control science and engineering from the National University of Defense Technology, Changsha, China, in 2021, where he is currently working toward the Ph.D. degree in management science and engineering. His current research focuses on crowdsensing, human-AI interaction, and intelligent transportation systems.

Chuan Ai received the Ph.D. degree in control science and engineering from the National University of Defense Technology, Changsha, China, in 2021. He is currently a lecturer with the College of Systems Engineering, National University of Defense Technology. His research interests include complex networks, information diffusion, and agent-based simulation.

Bin Chen received the Ph.D. degree in control science and engineering from the National University of Defense Technology, Changsha, China, in 2010. He is currently a professor with The Institute of Intelligent Computing, University of Electronic Science and Technology of China (UESTC). His research focuses on simulation intelligence and deep learning.

Zhengqiu Zhu received the Ph.D. degree in management science and engineering from National University of Defense Technology, Changsha, China, in 2023. He is currently a lecturer with the College of Systems Engineering, National University of Defense Technology. He has authored or coauthored more than 50 publications in international refereed journals and conferences. His research interests include source search, crowd computing, and embodied agents.